

# pH-Induced Volume-Phase Transition of Hydrogels Containing Sulfonamide Side Group by Reversible Crystal Formation

Seong Il Kang and You Han Bae\*

Center for Biomaterials and Biotechnology, Department of Materials Science and Engineering, Kwangju Institute of Science and Technology, 1 Oryong-dong, Puk-gu, Kwangju 500-712, Korea

Received December 27, 2000; Revised Manuscript Received August 24, 2001

**ABSTRACT:** Hydrogels composed of *N,N*-dimethylacrylamide and a sulfonamide monomer (SDM,  $pK_a = 6.17$ ) derived from sulfadimethoxine exhibited a pH-induced volume-phase transition in water. This resulted from pH-dependent ionization/deionization of the sulfonamide group and reversible side group crystallization (physical cross-linking). The pH-dependent equilibrium swelling pattern was controlled by the polymer composition. At higher SDM content, a higher transition pH and a larger and sharper transition were observed, leading to almost discontinuous swelling transition of a gel containing 40 mol % SDM around the physiological pH. It is evident that side group crystallization was primarily responsible for such a sharp transition, influenced by temperature-induced chain flexibility and associated with hydrogen bonding between un-ionized sulfonamide groups. However, after crystal melting at 70 °C, the pH dependency in swelling was well-preserved but with reduced sharpness, suggesting a partial role of hydrophobic interaction in the pH-induced volume-phase transition.

## Introduction

The coil–globule transition of soluble polymers or the volume-phase transition of cross-linked, swollen polymers by minute changes in environmental conditions, such as temperature,<sup>1,2</sup> light,<sup>3</sup> ionic strength,<sup>4</sup> and metabolite concentration,<sup>5</sup> has attracted great attention for its scientific interest and applications. Such transitions in an aqueous environment may provide a way to mimic the sensitive conformational changes of proteins. The volume-phase transitions in aqueous systems have been demonstrated by utilizing specific or nonspecific secondary interactions between polymer chains and solvent molecules<sup>6</sup> or between a ligand and a corresponding receptor.<sup>7,8</sup> Several types of volume-phase transition polymers based on sensitive secondary interactions, controlled by environmental conditions, were devised. A very recent version of the transition material was obtained by hybridization of a water-soluble polymer cross-linked with coiled-coil proteins.<sup>9</sup> The kinetic control of the swelling–shrinking of temperature-sensitive polymers by manipulating the topology of the network structure was also of interest.<sup>10</sup>

In this study, sulfadimethoxine (SD) [4-amino-*N*-(2,6-dimethoxy-4-pyrimidinyl)benzenesulfonamide], which has been known as an antibacterial agent for several decades,<sup>11</sup> was modified to a polymerizable monomer (SDM) through a reaction with methacryloyl chloride. The SDM was copolymerized with a water-soluble monomer, *N,N*-dimethylacrylamide, and a cross-linker, by a conventional free-radical solution polymerization method.

The sulfonamide family is known to have a pronounced tendency toward crystallization. The first observation of the crystallization and polymorphism of the sulfonamide family was reported by Zyp in 1938.<sup>12</sup> We report a volume-phase transition in swelling, particularly around the physiological pH, by reversible physical cross-linking junctions formed by the crystal-

lization of pendent sulfonamide groups in the chemically cross-linked gel. This finding adds a new phase transition polymer to known smart polymeric systems, which have been applied to various fields such as drug delivery, bioengineering, and biotechnology.

## Experimental Part

**Materials.** Sulfadimethoxine (SD) was purchased from Sigma (St. Louis, MO) and used as received. *N,N*-Dimethylacrylamide (DMAAm) and dimethyl sulfoxide (DMSO) from Aldrich (Milwaukee, WI) were purified by vacuum distillation at 20 °C/12 mmHg and 75 °C/12 mmHg, respectively. Methacryloyl chloride (Aldrich) was purified by vacuum distillation at 30 °C/10 mmHg. 2,2'-Azobis(isobutyronitrile) (AIBN; Acros, Geel, Belgium) was recrystallized from methanol (Acros) twice. *N,N*-Methylenebis(acrylamide) (MBAAm, Acros) and sodium hydroxide (Shinyo Pure Chemical, Japan) were all used as received.

**Monomer Synthesis.** Sulfadimethoxine monomer (SDM) was synthesized with SD and methacryloyl chloride. SD (10 mmol) and 10 mmol of sodium hydroxide were dissolved in aqueous acetone (40 mL, 1:1 v/v). Methacryloyl chloride (10 mmol) was then added drop by drop into the solution under vigorous stirring at 10 °C. The precipitated product was filtrated and dried in vacuo for 2 days at 25 °C. SDM was purified by recrystallization in methanol and washing with distilled water three times. The product was resuspended in methanol (10% w/v) and was stirred for 1 day to further extract SD. SDM was obtained by ultracentrifugation, filtration, and drying. For confirmation of structure and yield, <sup>1</sup>H NMR (JEOL JNM-LA 300 WB FT-NMR) was used. The purity of synthetic SDM calculated by peaks of NMR was over 99%.  $CH_2=C-CH_3$ : 5.6 ppm, 5.8 ppm;  $CH_2=C-CH_3$ : 1.9 ppm; CONH: 10.1 ppm; phenylene-*H*: 7.8 ppm; SONH: 11.5 ppm; pyrimidinyl-*H*: 6.7 ppm; pyrimidinyl N=C-OCH<sub>3</sub>: 2.2 ppm.

**pH-Dependent SDM Solubility.** The excess amount of SDM was added in a phosphate buffered solution (varying pH 6–11, 0.1 M ionic strength by NaCl). Each SDM suspension was kept in a shaking water bath thermostated at 37 ± 1 °C. After 2 weeks, undissolved SDM was isolated from the monomer-saturated supernatant by filtration through a cellulose acetate filter of pore size 0.20 μm. Spectrophotometric assay at 37 °C was carried out with a standard calibration curve using a Varian CARY 1E UV/vis spectrophotometer (He/Ne laser source) at a wavelength of 270 nm.<sup>13</sup>

\* To whom correspondence should be addressed. Tel +82-62-970-2305; Fax +82-62-970-2304; e-mail yhbbae@kjist.ac.kr.

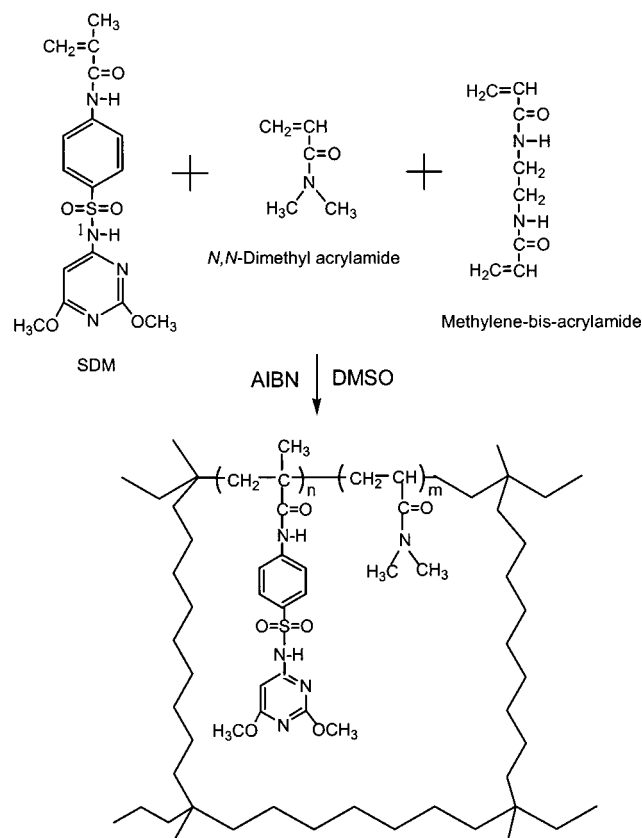


**Figure 1.** Chemical structures of gel components and the schematic structure of cross-linked poly(SDM-co-*N,N*-dimethylacrylamide).

**Synthesis of Cross-Linked Poly(SDM-co-DMAAm).** Cross-linked poly(SDM-co-DMAAm) with various compositions (10–40 mol % of SDM in feed) were synthesized by conventional radical polymerization. SDM, DMAAm, MBAAm (1 mol % of total monomers), and AIBN (0.2 mol % of monomers) were dissolved in DMSO (30% w/v monomer). After bubbling with dry nitrogen gas for 15 min, the monomer solution was injected into the area between two glass plates separated by a rubber spacer (3 mm in thickness). The mold was sealed and placed in a dry oven for 20 h at 65 °C. The chemical structure of the gel is presented in Figure 1. After polymerization, the polymer gel sheets were separated from the glass plates and punched into 1.2 cm diameter circular disks for swelling measurements or 4 mm diameter for X-ray diffraction study. All disks were washed in ethanol for 30 min and then soaked in aqueous sodium hydroxide solution (pH 8) for 1 week to extract all unreacted or low molecular weight compounds. The disks were then soaked in an aqueous hydrogen chloride solution (pH 3) for 1 day to neutralize them and then washed several times with deionized water. The samples were air-dried at room temperature for 3 days and further dried under vacuum at 40 °C for another 3 days. The resulting gels were named as GDSD10 (10 mol % SDM in feed), GDSD20 (20 mol %), GDSD30 (30 mol %), and GDSD40 (40 mol %).

**Equilibrium Swelling.** The equilibrium swellings of the gels at various pHs and temperatures were measured. After weighing, the dried gel disks were transferred into various pH buffer solutions (0.1 M ionic concentration) kept at a constant temperature and equilibrated for at least 2 days. The equilibration was confirmed by no weight change with time in the solution. The weight swelling ratio was calculated by  $(W_{\text{swollen}} - W_{\text{dry}})/W_{\text{dry}}$ , where  $W_{\text{swollen}}$  and  $W_{\text{dry}}$  are the weights of the swollen gel and dried gel, respectively.

**XRD Analysis.** The X-ray diffraction method was used to obtain diffraction diagrams of the samples (5 mm in diameter  $\times$  3 mm in thickness) at different pHs. X-ray diffractometric analyses were applied using a diffractometer equipped with a

Rigaku Denki RU-H3R system (Tokyo). Monochromic Cu K $\alpha$  radiation with  $\lambda = 15.4$  nm (40 kV and 200 mA) was used. For reversibility, the sample (GDSD30) was repeatedly equilibrated in two fixed pHs for 2 days at each pH (pH 7.4  $\rightarrow$  6.8  $\rightarrow$  7.4  $\rightarrow$  6.8 (two cycles)).

**DSC Analysis.** Melting points of GDSD30 were obtained by a differential scanning microcalorimetry (DSC; Hart Scientific TA 2050). The samples swollen in buffer solutions (pH 6.8 and 7.4) were scanned from 20 to 150 °C at a heating rate of 5 °C/min after removing surface water.

**Effective Cross-Linking Density.** Compression modulus and dried polymer density were employed to determine the apparent effective cross-linking densities of the gels. The density of the dried gel was determined by measuring gel volume in water using a hanging microbalance (Shimadzu, AX200). The unidirectional compression modulus of a swollen gel equilibrated at various pHs (pH 6.8 and 7.4) was measured using a compressor (IMIDA Co., Japan) at 25 °C. The same measurements of the gel equilibrated in the presence of 1 M urea were also carried out. The apparent effective cross-linking density was calculated by the equation of

$$\tau = RT \left( \frac{\phi_{p,0}}{\phi_p} \right)^{2/3} \phi_p \nu_e^* \left( \alpha - \frac{1}{\alpha^2} \right) \quad (1)$$

where  $\tau$  is the stress,  $R$  is the gas constant,  $T$  is the absolute temperature, and  $\phi_p$ ,  $\phi_{p,0}$  are the polymer volume fractions of the swollen polymer network during equilibrium swelling and relaxed states, respectively.  $\nu_e^*$  is the effective cross-linking density of the polymer network in the dried state, and  $\alpha$  is the linear deformation factor for the polymer network.

## Results and Discussion

### pH-Dependent SDM Solubility and Gel Swelling.

The synthesized monomer (SDM) was practically insoluble at low pH, and its solubility increased only slightly as the pH increased up to 6.6, followed by a sharp increase at higher pH. The sulfonamide group is readily ionizable at high pH because the strong electronegativity of the oxygen atoms of the sulfonyl group draws electrons from the sulfur atom, which in turn attracts electrons from the nitrogen atom ( $\text{N}^1$ , see Figure 1). The resulting electron deficiency of  $\text{N}^1$ -nitrogen makes the electrons of the  $\text{N}^1\text{—H}$  bond held to the nitrogen atom more closely, thus releasing the hydrogen of secondary amine at high pH and forming a negative ion ( $\text{N}^-$ ).<sup>11</sup> The  $\text{pK}_a$  of a sulfonamide compound is then governed by the electronic property of another attaching group to the nitrogen atom, such as the dimethoxypyrimidine group for SD.<sup>14</sup> Accordingly, the pH-dependent solubility curve (Figure 2a) for SDM shows a gradual increase in solubility as pH increases with an inflection point around pH 7.7. It is, however, noted that despite the  $\text{pK}_a$  of SD (known to be 6.10) and the measured  $\text{pK}_a$  of SDM from titration experiment being 6.17, almost no solubility of SDM around pH 6.2 (assuming  $\sim 50\%$  ionization of SDM) was found. This suggests that there might be certain interactions involved between ionized and un-ionized SMD in a solid state, preventing solubilization of ionized SDM until the population of ionized SDM becomes dominant.

Figure 2b shows the equilibrium swelling levels of the gels at different pH values at 37 °C. GDSD10 exhibited considerable swelling at low pH, and the swelling level gradually increased as the pH increased with an inflection point around pH 6.2, which is close to the  $\text{pK}_a$  value of SDM, reflecting minimal interactions between SDM residues in the network, probably due to its low density. The gels that synthesized with higher SDM content showed lower swelling levels at low pH, reaching a

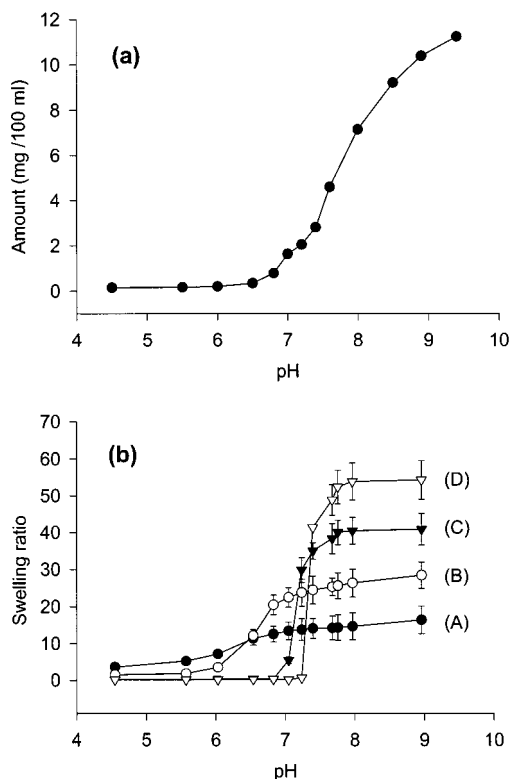


**Figure 2.** (a) pH-dependent SDM solubility at 37 °C and (b) pH-dependent equilibrium swelling ( $W_{\text{water}}/W_{\text{dried gel}}$ ) of the gels at 37 °C (A: GDSD10; B: GDSD20; C: GDSD30; D: GDSD40). A mean  $\pm$  s.d. ( $n = 5$ ).

completely collapsed state for GDSD30 and GDSD40, while their swelling levels at higher pH were remarkably elevated. The inflection point in the swelling curve shifted to higher pH (6.5 for GDSD20, 7.1 for GDSD30, and 7.3 for GDSD40), and the transition became sharper. For instance, the collapsed GDSD40 gel at pH 7.2 expanded to a swelling level of 40 at pH 7.4 (the 0.2 unit was the smallest change in pH in our experimental conditions), demonstrating that the swelling transition of GDSD40 gel became almost discontinuous. This observation further implies that there are increasing interactions between SDM residues in the networks as suspected in pH-dependent monomer solubility, affecting the swelling patterns of the gels.

The pH-dependent swelling of ionic gels is primarily attributed to the degree of ionization, generating ionic repulsion and osmotic pressure by counterions in the network.<sup>15</sup> However, the pH-dependent swelling behavior of GDSD gels observed in this study is clearly distinguished from those of conventional ionic gels, particularly the sharp transition and complete collapse for GDSD30 and 40 at low pH. The volume transition shown in Figure 2b cannot be explained simply by the degree of ionization of SDM, because conventional ionic gels based on sulfonic acid, carboxylic acid, or amino groups, of which the charge density in the networks varies gradually with pH, have not exhibited such transition in swelling, unless the polymers were considerably hydrophobized with water insoluble comonomers.<sup>16</sup> This is in contrast with the nature of the network prepared in this study where an hydrophilic comonomer of DMAAm was incorporated instead of a hydrophobic comonomer.

**XRD Analysis.** The hydrogen atom of H–N<sup>1</sup> may form a strong intermolecular hydrogen bond with the

oxygen atom of the (O=S=O) group in the sulfonamide. This hydrogen bonding is possibly further stabilized by van der Waals interaction with the surrounding phenyl group connected to the sulfonyl group and the residual group (R) attached to the nitrogen atom (N<sup>1</sup>), such as a dimethoxypyrimidine ring for SDM.<sup>17</sup> The two nitrogen atoms in the pyrimidine ring may also participate in hydrogen bonding with the secondary amine group. These interactions drive to crystallization of sulfonamide. The nature of the R group determines the structure of the crystal lattice. For instance, a sulfanilamide compound with (R = –NH<sub>2</sub>) formed an orthorhombic crystal with eight molecules in one unit cell.<sup>18</sup>

Against the expectation that the network structure may restrict the mobility of SDM side groups, hindering its packing tendency to a crystal form, the results of the X-ray diffraction study of the gels at two fixed pHs of 6.8 and 7.4 at 37 °C revealed that there was a remarkable crystallization of SDM in the network at pH 6.8 and the crystals dissolved at pH 7.4 (Figure 3a,b); two adjacent environmental pH values of 6.8 for a collapsed state and 7.4 for an expanded state were selected. As can be seen in Figure 3a, no crystallinity was observed for GDSD10, partial crystallinity for GDSD20, and high crystallinity for GDSD30 and GDSD40 which showed the collapsed state at pH 6.8.

In the wide-angle X-ray diffraction (WXR) spectra of GDSD30 and 40 gels kept at pH 6.8, it was found that a sharp peak appeared at  $2\theta = 12.6^\circ$  and two small peaks at  $9.4^\circ$  and  $19.8^\circ$ . The scattered vector ratios [wavelength (converted from  $2\theta$  values by Bragg equation) ratio of three peaks] of the three peaks coincide with those of the characteristics of triclinic structure which have been observed with SD.<sup>19</sup> The XRD at pH 7.4 showed no crystallinity in the gels (Figure 3b) but a broad amorphous water peak which may reflect the water content of the gels. When SD or SDM is in a free form in an aqueous environment at high pH, the acidic hydrogen in the secondary amine group dissociates, and the degree of dissociation is a function of pH. However, because the acidic hydrogen may be involved in hydrogen bonding to form a crystal structure, the water access to the sulfonamide groups in the crystal is greatly limited, minimizing the influence of environmental pH. When the pH reached a critical point, the crystallinity failed to resist the ionization of the hydrogen atom in the secondary amine, resulting in monomer solubility far above  $pK_a$  and gel expansion as seen in parts a and b of Figure 2, respectively. This result strongly supports the idea that the primary driving force for crystal formation of sulfonamide is hydrogen bonding.<sup>20</sup> The crystallinity allows the gel collapse at low pH because of the physical cross-linking effect of the crystals, in addition to the chemical cross-linking introduced when the gels were synthesized. The apparent effective cross-linking density was determined by measuring compression modulus of the gels, and the result is presented in Table 1. Effective cross-linking density reflects clearly the apparent interactions in the gel network. In the case of GDSD10 and -20, the effective cross-linking density was little affected by temperature and pH, while the effective cross-linking density at pH 6.8 increased 3.4–6.5 times for GDSD40 gel when compared with that measured at pH 7.4. This result suggests that the crystallization occurs above a critical population of sulfonamide residual groups in the network. The crystallization of sulfonamide groups in the gel may be



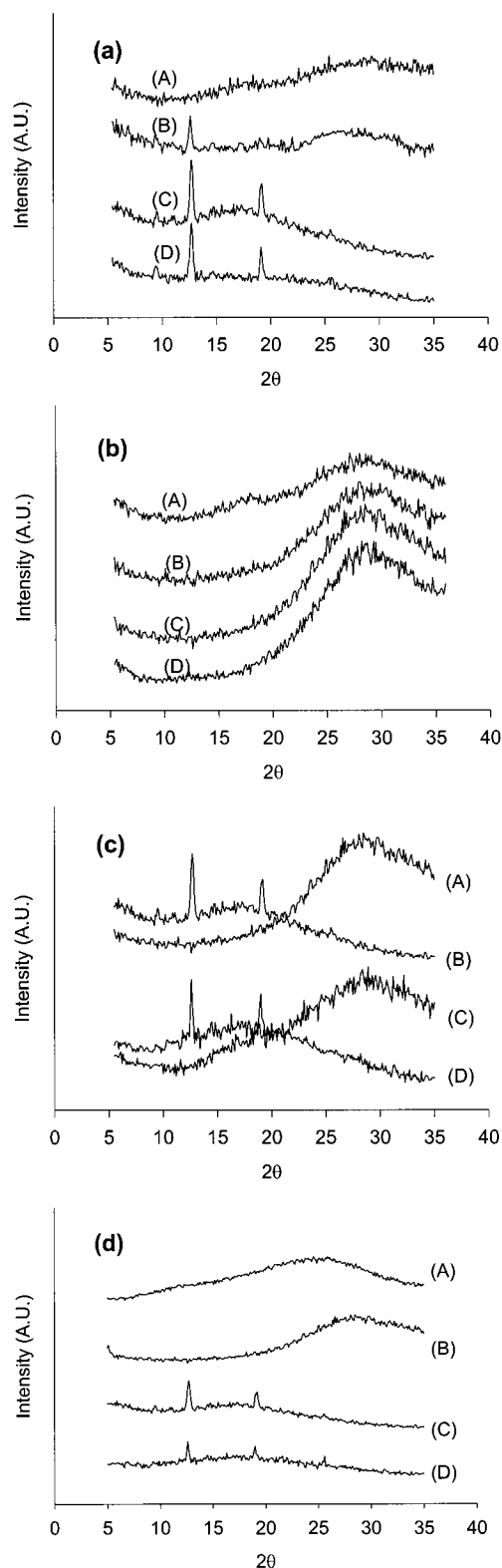


**Figure 3.** (a) XRD spectra for the gels at pH 6.8. (A: GDSD10; B: GDSD20; C: GDSD30; D: GDSD40). (b) XRD spectra for the gels at pH 7.4 (A: GDSD10; B: GDSD20; C: GDSD30; D: GDSD40). (c) Reversible crystal formation of GDSD30 at pH 7.4 and pH 6.8. The sample was repeatedly equilibrated at two fixed pHs for 2 days at each pH (pH 7.4  $\rightarrow$  6.8 (first cycle)  $\rightarrow$  7.4  $\rightarrow$  6.8 (second cycle)). A: X-ray spectrum at pH 7.4 from the first cycle. B: X-ray spectrum at pH 6.8 from the first cycle. C: X-ray spectrum at pH 7.4 from the second cycle. D: X-ray spectrum at pH 6.8 from the second cycle. (d) XRD spectra of GDSD30 at 37 °C and different pHs (A: pH 9.0; B: pH 7.0; C: pH 5.0; D: pH 3.0).

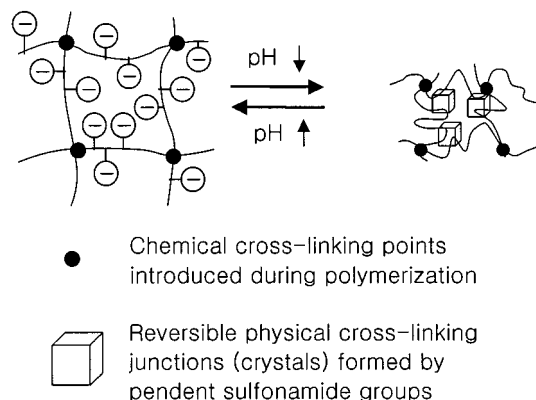


**Figure 4.** Schematic illustration for reversible crystal formation in the gel which caused volume-phase transition. The polymer gel expands when the sulfonamide groups are fully negatively charged at high pH and completely collapse by protonation of sulfonamide groups at low pH and subsequent crystallization.

responsible for the sharp transition in the swelling of the GDSD30 and GDSD40.

The crystallization was reversible when the gel was repeatedly exposed to pH 6.8 and 7.4, as demonstrated in Figure 3c. Figure 3d also shows the pH-dependent crystallization of GDSD30 at 37 °C. It again suggests that the deionization of secondary amine plays a leading role in crystal formation. A possible structural change of the gel caused by the crystallization, thus influencing pH-dependent swelling behavior, is depicted in Figure 4.

**Temperature Effect on Swelling and Crystallization.** For better understanding of the swelling behavior of the gels and associated interactions in the gels, we have selected a gel of GDSD30, which showed less sensitivity to pH than GDSD40. The results for investigation of temperature effect on pH-dependent equilibrium swelling are given in Figure 5. A three-dimensional diagram (swelling–temperature–pH) was constructed in Figure 5a, and two two-dimensional diagrams (Figure 5b for swelling–temperature and Figure 5c for swelling–pH) are presented to help visualization. As can be seen in Figure 5b, the gel exhibits temperature-dependent swelling at a specific pH range of 6.8–7.4. Below pH 6.5, the gel showed practically no swelling at all temperatures except 70 °C, which was assigned as a crystal melting temperature. The crystal melting endotherm was observed by DSC as presented in Figure 6 (line A) with a peak around 70 °C, but without a water melting peak, indicating that no free water exists in the gel in these conditions. On the other hand, when the gel was equilibrated at pH 7.4, no crystal melting peak was observed, but there was a broad water melting peak (Figure 6, line B). The crystal melting by temperature below pH 7.0 caused an increase in swelling, the degree of which depended on the pH. The melting effect was most significant at pHs 6.8 and 7.0. The melted and un-ionized SDM may still form hydrophobic clusters preventing gel expansion, and the hydrophobic interaction was reduced by ionization as the pH value became higher. This observation suggests again that the crystallinity in the gel helps the gel to keep a collapsed state and the swelling is not influenced by temperatures below the crystal melting point.<sup>18</sup>

The positive thermosensitivity in swelling, i.e., higher swelling at elevated temperature, is a typical charac-

**Table 1.** Apparent Effective Cross-Linking Densities of GDSD Gels at pH 6.8 and 7.4

	GDSD1	GDSD2	GDSD3	GDSD4
effective cross-linking density at pH 6.8 (mol/cm <sup>3</sup> )	$3.41 \times 10^{-8}$	$3.56 \times 10^{-8}$	$2.26 \times 10^{-7}$	$2.29 \times 10^{-7}$
Effective cross-linking density at pH 7.4 (mol/cm <sup>3</sup> )	$3.47 \times 10^{-8}$	$3.38 \times 10^{-8}$	$3.10 \times 10^{-8}$	$3.26 \times 10^{-8}$

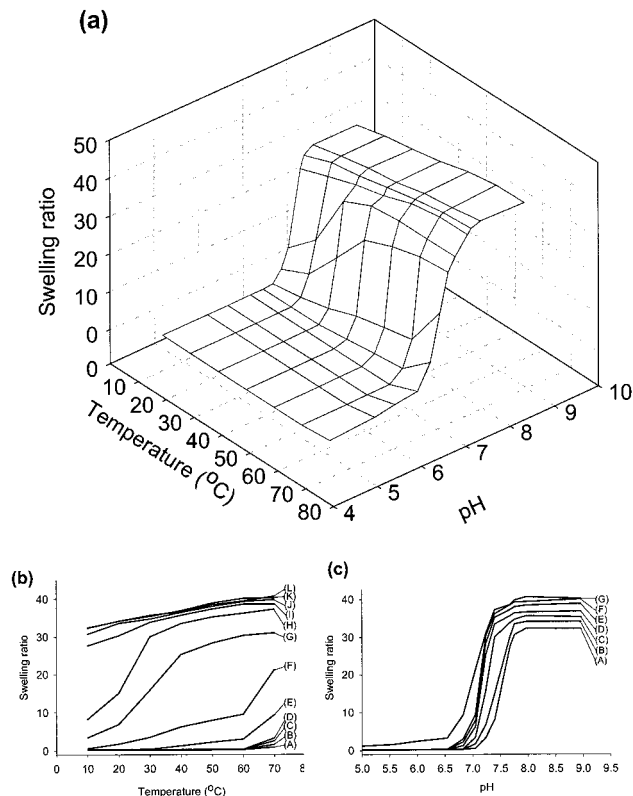


**Figure 5.** (a) Three-dimensional diagram of GDSD30 equilibrium swelling as functions of pH and temperature. (b) Temperature-dependent swelling of GDSD30 at various pHs (A: pH 4.55; B: pH 5.57; C: pH 6.03; D: pH 6.54; E: pH 6.83; F: pH 7.05; G: pH 7.24; H: pH 7.40; I: pH 7.68; J: pH 7.76; K: pH 7.97; L: pH 8.96). (c) pH-dependent swelling of GDSD30 at various temperatures (A: 10 °C; B: 20 °C; C: 30 °C; D: 40 °C; E: 50 °C; F: 60 °C; G: 70 °C).

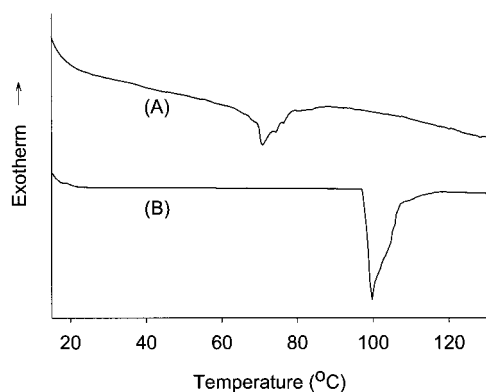


**Figure 6.** DSC thermogram of GDSD30. The samples were equilibrated at (A) pH 6.8 and (B) pH 7.4.

teristic of the temperature-dependent swelling pattern of hydrogel networks where the inter- and intrachain interactions are governed by hydrogen bonding.<sup>2,21</sup> The positive thermosensitivity for the gel observed around the neutral pH region suggests that although the crystallinity in the gel is totally disturbed by the ionization, there still remained strong hydrogen-bonding interaction among SDM and between SDM and DMAAm in the network, and this interaction became weakened

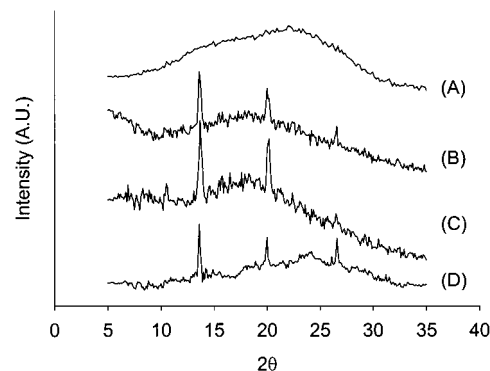


**Figure 7.** XRD spectra for GDSD30 at pH 6.8 and different temperatures (A: 70 °C; B: 50 °C; C: 30 °C; D: 10 °C).

as the pH increased, thus by higher degrees of ionization, as indicated by the shift of inflection point in a temperature-dependent swelling curve to a lower temperature. Above pH 7.7, no significant hydrogen-bonding effect on swelling was found. It is interesting to note that the hydrogen-bonding effect was minimal at physiological conditions (37 °C and pH 7.4) but became significant below pH 7.0 at the tested temperature range.

The temperature effect on pH-dependent swelling is shown in Figure 5c. One characteristic feature is that at the middle temperature range (30–60 °C) the pH-induced swelling transition is sharper than those after crystal melting (70 °C) and at the low-temperature range (below 20 °C). Another feature is that the transition pH (inflection point in swelling curve) shifted from pH 7.5 to 7.0 as the temperature increased from 10 to 70 °C. The transition sharpness and transition pH remained almost unchanged at 40, 50, and 60 °C. The temperature effect at the higher pH region above pH 8.0 may be attributed to the solvation power of water with increasing thermal energy. One possible explanation for the shift of transition pH may be the van't Hoff effect, more ionization tendency at higher temperature.<sup>22</sup>

The transition sharpness seems to be closely associated with temperature-dependent crystal formation as seen in Figure 7. The XRD data revealed that the crystal peaks at 10 °C are apparent but less intense than those at 30 and 50 °C, and there is no crystallinity at 70 °C by crystal melting. Although crystallization is thermodynamically favored at low temperature, the observed poor crystallinity in the gel at 10 °C may be attributed to the reduced hydrophobic interaction and polymer chain flexibility (kinetic hindrance). This result indirectly indicates that the chain flexibility for proper side chain reorientation seems to be an important factor in determining the process of crystallization in the network.<sup>23</sup> Indeed, when the network was heavily cross-linked during synthesis by the chemical cross-linking reaction (more than 8 mol % of the cross-linker in feed composition), thus restricting chain mobility, no crystal was formed under any condition (data are not shown).

Because the gel with no crystallinity by melting showed pH sensitivity as well, possibly due to strong hydrophobic interaction among deionized SDM, the

crystallinity is not solely responsible for the pH dependency of the gel. However, the crystallinity definitely contributes to the sharpness in the pH-induced swelling transition curve, which then leads to an almost discontinuous swelling transition for GDSD40 having a higher degree of crystallinity in the network.

The pH-induced volume transition of gels is expected to be a base of soft smart materials for various applications including the soft actuator, molecular valves, sensors, and separation.<sup>24–27</sup> The smart polymers are also expected to work as drug carriers for targeting minute changes in pH in the body, such as tumor tissues,<sup>28</sup> and for triggered or self-regulated drug release.<sup>29</sup>

## Conclusion

The pH-induced volume-phase transition of polymer gels containing sulfonamide pendent groups occurred by ionization/deionization, hydrophobic interaction of deionized groups, and reversible crystal formation of the side groups in the network structure. The transition pattern was controlled by the polymer composition. At higher SDM content, a higher transition pH and a sharper transition were observed, leading to almost discontinuous swelling transition around the physiological pH. This feature was mainly associated with the crystallization of the side sulfonamide groups. Temperature seems to be one of the important factors in determining the side chain crystallization process by providing sufficient chain flexibility for reorientation of the side groups.

**Acknowledgment.** This work was supported by KOSEF through the Hyperstructured Organic Materials Center and by the BK21 project.

## References and Notes

- (1) Chen, G.; Hoffman, A. S. *Nature* **1995**, *37*, 49.
- (2) Matsuo, E. S.; Tanaka, T. *Nature* **1992**, *358*, 482.
- (3) Karibayants, N.; Dautzenberg, H.; Colfen, H. *Macromolecules* **1997**, *30*, 7803.
- (4) Suzuki, A.; Tanaka, T. *Nature* **1990**, *346*, 345.
- (5) Cartier, S.; Horbett, T. A.; Ratner, B. D. *J. Membr. Sci.* **1995**, *106*, 17.
- (6) Ilmain, F.; Tanaka, T.; Kokufuta, E. *Nature* **1991**, *349*, 400.
- (7) Kiser, P. F.; Wilson, G.; Needham, D. *Nature* **1998**, *394*, 459.
- (8) Miyata, T.; Assami, N.; Uragami, T. *Nature* **1999**, *399*, 766.
- (9) Wang, C.; Stewart, R. J.; Kopecek, J. *Nature* **1999**, *397*, 417.
- (10) Yoshida, R.; et al. *Nature* **1995**, *374*, 240.
- (11) Bell, P. H.; Richard, O.; Robin, J. R. *J. Am. Chem. Soc.* **1942**, *64*, 2905.
- (12) O'Connor, B. H.; Maslen, E. N. *Acta Crystallogr.* **1965**, *18*, 363.
- (13) Hampson, J. W.; Maxwell, R. J.; Li, S.; Shadwell, R. J. *J. Chem. Eng. Data* **1999**, *44*, 1222.
- (14) Cammarata, A.; Allen, R. C. *J. Pharm. Sci.* **1967**, *56*, 640.
- (15) Bronsted, H.; Kopecek, J. *pH-Sensitive Hydrogels. Polyelectrolyte Gels*; Harland, R. S., Prudhomme, R. K., Eds.; ACS Symposium Series 480; American Chemical Society: Washington, DC, 1992; pp 285–304.
- (16) Philippova, O. E.; Hourdet, D.; Audebert, R.; Khokhlov, A. R. *Macromolecules* **1996**, *29*, 2822.
- (17) Foernzler, E. C.; Martin, A. N. *J. Pharm. Sci.* **1967**, *56*, 608.
- (18) Yang, S. S.; Guillory, J. K. *J. Pharm. Sci.* **1972**, *61*, 26.
- (19) Narula, P.; Haridas, M.; Singh, T. P. *Indian J. Phys.* **1987**, *61*, 132.
- (20) Patel, U.; Tiwari, R. T.; Patel, T. C.; Singh, T. P. *Indian J. Phys.* **1983**, *57*, 90.
- (21) Katono, H.; Maruyama, A.; Sanui, K.; Ogata, N.; Okano, T.; Sakurai, Y. *J. Controlled Release* **1991**, *16*, 215.
- (22) Atkins, P. W. *Physical Chemistry*; Oxford University Press: Oxford, 1995; p 877.
- (23) Deanin, R. D. *Polymer Structure, Properties and Applications*; Cahnners Books: Boston, 1972; p 214.
- (24) Snowden, M. J.; Murray, M. J.; Chowdry, B. Z. *Chem. Ind.* **1996**, *15*, 531.
- (25) Ichijo, H.; Kishi, R.; Hirasa, O. *Biotechnol. Bioeng.* **1994**, *2*, 315.
- (26) Bae, Y. H.; Okano, T.; Kim, S. W. *J. Polym. Sci., Part B: Polym. Phys.* **1990**, *28*, 923.
- (27) Davies, M. L.; Hamilton, C. J.; Murphy, S. M.; Tigie, B. J. *Biomaterials* **1992**, *13*, 971.
- (28) Berg, A. P. V. D.; Hooley, J. L. W.; Berg-Blok, A. E. V. D.; Zee, J. V. D.; Reihold, H. S. *Eur. J. Cancer* **1982**, *18*, 457.
- (29) Hassan, C. M.; Doyle III, F. J.; Peppas, N. A. *Macromolecules* **1997**, *30*, 6166.

MA0021949